

## Two measurements of the $^{22}\text{Na}+p$ resonant scattering via thick-target inverse-kinematics method

Y.B. Wang<sup>1,a</sup>, S.J. Jin<sup>1</sup>, L. Jing<sup>1</sup>, Z.Y. Han<sup>1</sup>, X.X. Bai<sup>1</sup>, B. Guo<sup>1</sup>, Y.J. Li<sup>1</sup>, Z.H. Li<sup>1</sup>, G. Lian<sup>1</sup>, J. Su<sup>1</sup>, L.J. Sun<sup>1</sup>, S.Q. Yan<sup>1</sup>, S. Zeng<sup>1</sup>, W.P. Liu<sup>1</sup>, H. Yamaguchi<sup>2</sup>, S. Kubono<sup>2</sup>, J. Hu<sup>2,3</sup>, D. Kahl<sup>2</sup>, J.J. He<sup>3</sup>, J.S. Wang<sup>3</sup>, X.D. Tang<sup>3</sup>, S.W. Xu<sup>3</sup>, P. Ma<sup>3</sup>, N.T. Zhang<sup>3</sup>, Z. Bai<sup>3</sup>, M.R. Huang<sup>3</sup>, B.L. Jia<sup>3</sup>, S.L. Jin<sup>3</sup>, J.B. Ma<sup>3</sup>, S.B. Ma<sup>3</sup>, W.H. Ma<sup>3</sup>, Y.Y. Yang<sup>3</sup>, L.Y. Zhang<sup>3</sup>, H.S. Jung<sup>4</sup>, J.Y. Moon<sup>4</sup>, C.S. Lee<sup>4</sup>, T. Teranishi<sup>5</sup>, H.W. Wang<sup>6</sup>, H. Ishiyama<sup>7</sup>, N. Iwasa<sup>8</sup>, T. Komatsubara<sup>9</sup>, and B.A. Brown<sup>10</sup>

<sup>1</sup>China Institute of Atomic Energy, Beijing 102413, China

<sup>2</sup>Center for Nuclear Study(CNS), University of Tokyo, Saitama 351-0198, Japan

<sup>3</sup>Institute of Modern Physics, Chinese Academy of Sciences, Lanzhou 730000, China

<sup>4</sup>Chung-Ang University, Seoul 156-756, Republic of Korea

<sup>5</sup>Kyushu University, Fukuoka 812-8581, Japan

<sup>6</sup>Shanghai Institute of Applied Physics, Chinese Academy of Sciences, Shanghai 201800, China

<sup>7</sup>High Energy Accelerator Research Organization(KEK), Ibaraki 305-0801, Japan

<sup>8</sup>Tohoku University, Miyagi 980-8578, Japan

<sup>9</sup>University of Tsukuba, Ibaraki 305-8571, Japan

<sup>10</sup>Michigan State University, East Lansing, Michigan 48824-1321, USA

**Abstract.**  $^{22}\text{Na}$  is an important isotope for the study of extinct radioactivity, meanwhile its sufficiently long half life provides the possibility to observe live  $^{22}\text{Na}$  in nearby nova explosions. The  $^{22}\text{Na}(p,\gamma)^{23}\text{Mg}$  is one of the key reactions that influence the  $^{22}\text{Na}$  abundance in nova ejecta. To study the proton resonant states in  $^{23}\text{Mg}$  relevant to the astrophysical  $^{22}\text{Na}(p,\gamma)^{23}\text{Mg}$  reaction rates, two measurements have been carried out at the CRIB separator of University of Tokyo, and the RIBLL secondary beamline in Lanzhou, respectively. The  $^{22}\text{Na}$  secondary beam was produced via the  $^1\text{H}(^{22}\text{Ne}, ^{22}\text{Na})n$  charge exchange reaction. Thick-target inverse-kinematics method is applied to obtain the excitation function of  $^{22}\text{Na}+p$  elastic scattering. Extended gas target and solid state polyethylene foil were used in the two measurements, respectively, to map the different excitation energy region of the compound nucleus  $^{23}\text{Mg}$ . Several new resonant levels are observed and their contribution to the  $^{22}\text{Na}(p,\gamma)^{23}\text{Mg}$  reaction rate is evaluated.

## 1 Introduction

Cosmic  $\gamma$  ray is a powerful tool to trace and locate new cosmic events. Great progress in the field of  $\gamma$ -ray astronomy has been achieved in the past twenty years, brought largely by the Compton Gamma Ray Observatory (CGRO) of NASA [1], and the International Gamma Ray Astrophysics Laboratory(INTEGRAL) of European Space Agency [2]. The main motivation of these missions is to

<sup>a</sup>e-mail: ybwang@ciae.ac.cn

observe cosmic  $\gamma$  rays from the decay of relatively long-lived  ${}^7\text{Be}$ ,  ${}^{18}\text{F}$ ,  ${}^{22}\text{Na}$ ,  ${}^{26}\text{Al}$ ,  ${}^{44}\text{Ti}$  and  ${}^{60}\text{Fe}$  isotopes.  ${}^{22}\text{Na}$  has a half life of 2.6 y, and it decays to the first excited state of  ${}^{22}\text{Ne}$  which emits a 1.275 MeV characteristic  $\gamma$  ray. The stellar sources of radioactive  ${}^{22}\text{Na}$  are primarily created in neon-rich nova [3, 4] and supernova explosions [5, 6]. In neon-rich novae, the  ${}^{22}\text{Na}$  is produced by the so-called high-temperature NeNa-MgAl reaction sequences [7, 8], *i.e.*  ${}^{20}\text{Ne}(p, \gamma){}^{21}\text{Na}(\beta^+){}^{21}\text{Ne}(p, \gamma){}^{22}\text{Na}$ , or  ${}^{20}\text{Ne}(p, \gamma){}^{21}\text{Na}(p, \gamma){}^{22}\text{Mg}(\beta^+){}^{22}\text{Na}$  alternatively. In 1972, an extraordinarily large  ${}^{22}\text{Ne}/{}^{20}\text{Ne}$  abundance ratio or nearly pure  ${}^{22}\text{Ne}$  was found in low-density graphite grains separated from carbonaceous meteorites [9], which indicates the extinct radioactivity of  ${}^{22}\text{Na}$  [10]. In 1974, Clayton and Hoyle predicted the possibility to observe live  ${}^{22}\text{Na}$  by the 1.275 MeV  $\gamma$  ray from nearby classical nova explosions [11]. The COMPTEL experiments on board CGRO observed five recent Ne-type novae, which resulted in an upper limit of  $3.7 \times 10^{-8} M_{\odot}$  of  ${}^{22}\text{Na}$  ejected by any nova in the Galactic disk [12]. Comparing to its relatively long half life, the main depletion mechanism of  ${}^{22}\text{Na}$  is through the  ${}^{22}\text{Na}(p, \gamma){}^{23}\text{Mg}$  reaction, the reaction rate over a large range of temperatures is thus crucial in deriving ranges of  ${}^{22}\text{Na}$  production during nova and supernova outbursts.

Many experimental investigations have been carried out to reduce the uncertainties of the  ${}^{22}\text{Na}(p, \gamma){}^{23}\text{Mg}$  reaction rate, including direct measurements of the reaction rate with radioactive  ${}^{22}\text{Na}$  targets [13–16], or indirect measurements for  ${}^{23}\text{Mg}$  resonance properties via the  $\beta$  decay of  ${}^{23}\text{Al}$  [17–20], and various transfer [21–23] or fusion-evaporation [24, 25] reactions. In these studies new  ${}^{23}\text{Mg}$  levels were identified in the energy region of astrophysical interest. However, most of the spectroscopic information is still missing due to the very complicated level structure of odd-mass  ${}^{23}\text{Mg}$  close to the proton threshold. The  ${}^{22}\text{Na}+p$  entrance channel is sensitive to populate the  ${}^{23}\text{Mg}$  proton resonance states relevant to the  ${}^{22}\text{Na}(p, \gamma){}^{23}\text{Mg}$  reaction; while thick target inverse kinematics (TTIK) technique [26] facilitates the measurement of the excitation function of  ${}^{22}\text{Na}(p, p)$  elastic scattering. Crucial resonant parameters of  ${}^{23}\text{Mg}$  can then be deduced for the evaluation of the  ${}^{22}\text{Na}(p, \gamma){}^{23}\text{Mg}$  reaction rate.

## 2 Experiment

Two measurements using thick-target inverse kinematics method were carried out with intense radioactive  ${}^{22}\text{Na}$  beams of different energies. Extended gas target and solid state polyethylene foil were used in the two measurements, respectively, to map the different excitation energy region of the compound nucleus  ${}^{23}\text{Mg}$ .

### 2.1 CRIB experiment

One experiment was carried out at the CNS radioactive ion beam separator (CRIB) [27, 28] of the University of Tokyo located in the RIKEN radioactive ion beam factory (RIBF). CRIB is a low-energy in-flight separator which can deliver intense secondary beams of low- and medium-mass nuclei. In the experiment  ${}^{22}\text{Na}$  was produced via the  ${}^1\text{H}({}^{22}\text{Ne}, {}^{22}\text{Na})\text{n}$  reaction. The  ${}^{22}\text{Ne}$  primary beam of 6.0 AMeV bombarded in a hydrogen gas cell of 80 mm in length, which was confined by Havar foils of  $2.5 \mu\text{m}$  in thickness and cooled with liquid nitrogen to a temperature of about 90 K. A nearly pure  ${}^{22}\text{Na}$  beam was delivered to the  ${}^{22}\text{Na}+p$  resonant scattering with an intensity of about  $2.5 \times 10^5$  pps.

The  ${}^{22}\text{Na}$  beam particles were monitored by two parallel-plate avalanche counters (PPACs) before reaching the secondary hydrogen target. The secondary gas target is semi-cylindrical in shape with a length of 300 mm. The energy of the  ${}^{22}\text{Na}$  secondary beam after the entrance window of the gas target was  $37.1 \pm 1.0$  MeV. During the  ${}^{22}\text{Na}+p$  measurement, the hydrogen gas target was maintained within  $310 \pm 2$  Torr by a gas-flow system; this pressure was chosen to fully stop the  ${}^{22}\text{Na}$  particles

in the gas volume. The lighter recoil particles emerging from the exit window were detected by a silicon-detector telescope (ST) centered at  $\theta_{\text{lab}} = 0^\circ$ . The ST consists of  $\Delta E$  and  $E$  layers, where the  $\Delta E$  layer is a double-sided silicon strip detector (DSSD) with orthogonally oriented  $16 \times 16$  readout strips on both sides and the  $E$  layer is a single-pad silicon detector. All the silicon detectors have an area of  $50 \text{ mm} \times 50 \text{ mm}$ . The thickness of the  $\Delta E$  detector is  $75 \mu\text{m}$  and that of the  $E$  detectors is about  $1.5 \text{ mm}$ .

## 2.2 RIBLL experiment

The radioactive ion beam line in Lanzhou (RIBLL) is primarily a double-achromatic anti-symmetry fragment separator [29], which is constructed at the heavy ion research facility of Lanzhou (HIRFL). The operation of RIBLL has been mainly based on the coupling of two cyclotrons together, *i.e.* a  $K=69$  Sector Focus Cyclotron (SFC) for low-energy ions and a  $K=450$  Separate Sector Cyclotron (SSC) for intermediate-energy ions. In order to obtain low-energy intense secondary beams by transfer reaction, a setup similar to CRIB was recently installed including a gas target system at the entrance position of RIBLL [30]. The new setup enables the primary beam from SFC to be transported directly to RIBLL, *i.e.* to bombard the gas target system. The secondary ions are subsequently separated and delivered by the 35 m-long RIBLL separator.

The production condition for  $^{22}\text{Na}$  secondary beam is similar to that of the CRIB experiment. The  $^{22}\text{Ne}$  primary beam of  $7.5 \text{ AMeV}$  bombarded in a hydrogen gas cell of  $80 \text{ mm}$  in length, which was confined by Havar foils of  $2.5 \mu\text{m}$  in thickness and cooled with alcohol to a temperature of about  $0^\circ\text{C}$ . The  $^{22}\text{Na}$  secondary beam was monitored by a time-of-flight (TOF) system made of two plastic scintillators, and by two PPACs in the flight path. A schematic layout of the experimental setup for the  $^{22}\text{Na} + p$  resonant scattering is shown in Fig. 1. In the target position, a polyethylene foil of  $100 \mu\text{m}$  in thickness served as the reaction target, while a  $61 \mu\text{m}$  thick carbon foil was used to evaluate the background. On the same slide, a single-pad silicon detector was also installed for the beam-tuning runs. Downstream from the target, the detector setup for lighter recoil particles is similar to that of the previous CRIB experiment. For the  $\Delta E$  layer at  $\theta_{\text{lab}} = 0^\circ$ , a larger DSSD with an area of  $70 \text{ mm} \times 70 \text{ mm}$  was used, which has  $32 \times 32$  readout strips on both sides. During the experiment, a nearly pure  $^{22}\text{Na}$  beam was delivered with an intensity of about  $8.5 \times 10^4 \text{ pps}$ . The energy of the  $^{22}\text{Na}$  secondary beam on the surface of the  $(\text{CH}_2)_n$  target was  $93.3 \pm 1.4 \text{ MeV}$ .

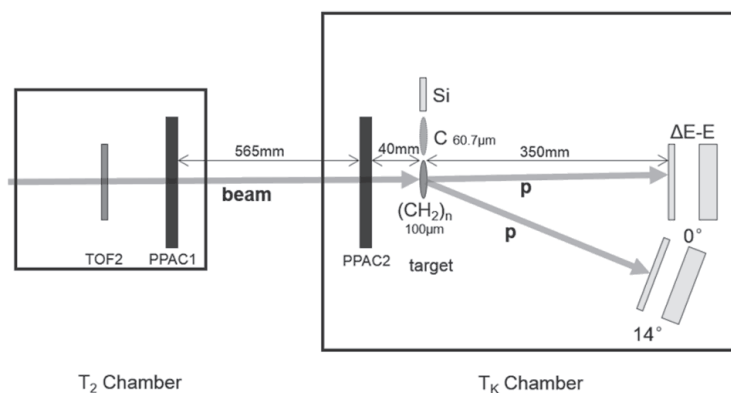


**Figure 1.** Schematic layout of the experimental setup for the  $^{22}\text{Na} + p$  resonant scattering at RIBLL.

### 3 Results

The complexity in the analysis of a thick-target experimental data lies in the fact that at any individual angle, the proton energy spectrum is continuous over a certain range. By taking the two-body kinematics of  ${}^1\text{H}({}^{22}\text{Na}, p){}^{22}\text{Na}$  elastic scattering and by considering the energy losses of  ${}^{22}\text{Na}$  and proton along their trajectories, the  $E_{\text{c.m.}}$  was deduced from the detected proton total energy on an event-by-event basis. After the conversion, the proton yields were added up over different  $\theta_{\text{lab}}$  defined by each pixel of the DSSD. The laboratory averaged differential cross section for the  ${}^{22}\text{Na} + p$  elastic scattering is deduced from the net proton yield according to

$$\left(\frac{d\sigma}{d\Omega}\right)_{\text{lab}} = \frac{\frac{dN_p}{dE}}{I_{\text{beam}} \frac{dN_t}{dE} d\Omega}, \quad (1)$$

where  $dN_p/dE$  refers to the net proton yield per  $E_{\text{c.m.}}$  unit,  $dN_t/dE$  is the energy dependent number of hydrogen atoms,  $I_{\text{beam}}$  is the total number of incident  ${}^{22}\text{Na}$  particles, and  $d\Omega$  is the solid angle. The differential cross section in the center-of-mass frame is obtained by

$$\left(\frac{d\sigma}{d\Omega}\right)_{\text{c.m.}} = \frac{1}{4 \cos \theta_0} \left(\frac{d\sigma}{d\Omega}\right)_{\text{lab}}, \quad (2)$$

where  $\theta_0$  is the averaged laboratory scattering angle.

For the CRIB experiment, the excitation function of the  ${}^{22}\text{Na}(p, p)$  elastic scattering and the  $R$ -matrix analysis have been published in Ref. [31]. Due to the stopping power of the gas target, the excitation function for the  ${}^{22}\text{Na}(p, p)$  elastic scattering is obtained over a small range of excitation energies, as shown in Fig. 2. Three peaks have been observed at  $E_R = 1.030$ , 1.212 and 1.335 MeV in the excitation function. The best  $R$ -matrix fit to the excitation function includes three resonances with  $J^\pi = (5/2 \text{ to } 9/2)^-, 7/2^+$  and  $5/2^+$ , respectively. The proton partial widths of the observed  ${}^{23}\text{Mg}$  states are also deduced from the  $R$ -matrix analysis. The explicit assignments of the spin and parity to the 8.793 and 8.916 MeV resonances in  ${}^{23}\text{Mg}$  allow for the shell-model calculation of the proton spectroscopic factors and the  $\gamma$  widths. Based on the resonant parameters obtained in this work, the  ${}^{22}\text{Na}(p, \gamma){}^{23}\text{Mg}$  reaction rate is re-evaluated. An enhancement of about 5% over the evaluation by NACRE [32] is found for  $T_9 > 2$  owing to the two new  $s$ -wave resonant states.

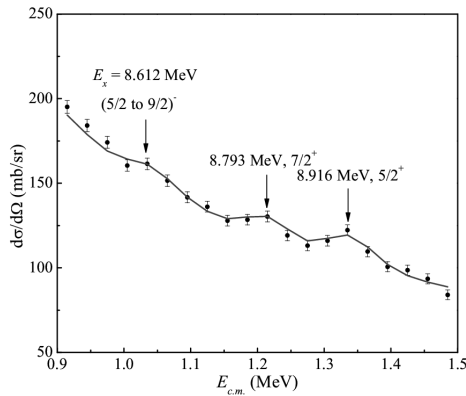


**Figure 2.** Excitation function for the  ${}^{22}\text{Na}(p, p)$  elastic scattering obtained from the CRIB experiment.

For the RIBLL experiment, a similar data analysis has been performed and a preliminary excitation function for the  $^{22}\text{Na}(p, p)$  elastic scattering is shown in Fig. 3. By using a higher-energy  $^{22}\text{Na}$  beam and a solid-state  $(\text{CH}_2)_n$  target, the excitation function for the  $^{22}\text{Na}(p, p)$  elastic scattering could be extended up to  $E_{c.m.} \approx 4$  MeV, quite complicated resonance structure is observed for further decomposition by  $R$ -matrix analysis.

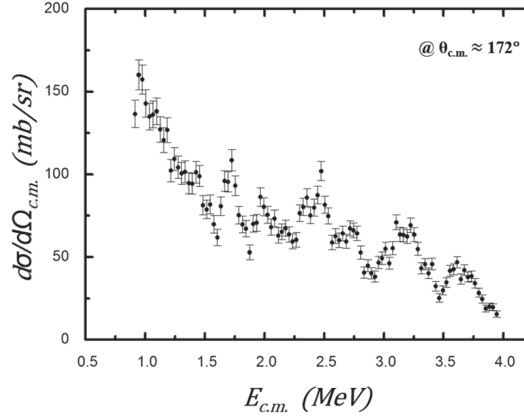


**Figure 3.** Preliminary excitation function for the  $^{22}\text{Na}(p, p)$  elastic scattering obtained from the recent RIBLL experiment.

## 4 Summary

The  $^{22}\text{Na} + p$  resonant scattering has been studied via the thick-target inverse-kinematics method with gas and solid-state targets at different  $^{22}\text{Na}$  beam energies. Excitation function for the  $^{22}\text{Na}(p, p)$  elastic scattering is extended up to  $E_{c.m.} \approx 4$  MeV, corresponding to an excitation energy of about 11.6 MeV in  $^{23}\text{Mg}$ . Complicated resonance structure is observed, which indicates the possibility to explore new proton resonance levels in  $^{23}\text{Mg}$  relevant to the  $^{22}\text{Na}(p, \gamma)^{23}\text{Mg}$  and  $^{19}\text{Ne}(\alpha, p)^{22}\text{Na}$  reactions. The present work demonstrates that resonance parameters of astrophysical significance can be directly obtained by using the thick-target inverse-kinematics method with secondary beams.

## Acknowledgments

This work was performed at the RI Beam Factory operated by RIKEN Nishina Center and CNS, the University of Tokyo, and at the heavy ion research facility of Lanzhou, respectively. The authors are grateful to the RIKEN and HIRFL accelerator staff for the smooth operation of the machines. This work is supported by the National Natural Science Foundation of China under Grant Nos. 11021504, 11175261, 11327508 and the 973 Program of China under Grant No. 2013CB834406, as well as by the JSPS KAKENHI (No. 21340053) and the Priority Centers Research Program in Korea (No. 2009-0093817).

## References

- [1] CGRO, <http://science.nasa.gov/missions/cgro>.

- [2] INTEGRAL, <http://sci.esa.int/integral>.
- [3] S. Amari, X. Gao, L. R. Nittler *et al.*, *Astrophys. J.* **551**, 1065 (2001).
- [4] J. José, M. Hernanz, S. Amari *et al.*, *Astrophys. J.* **612**, 414 (2004).
- [5] S. Amari, *Astrophys. J.* **690**, 1424 (2009).
- [6] P. R. Heck, S. Amari, P. Hoppe *et al.*, *Astrophys. J.* **701**, 1415 (2009).
- [7] M. Arnould and H. Nørgaard, *Astron. Astrophys.* **64**, 195 (1978).
- [8] J. José, A. Coc, and M. Hernanz, *Astrophys. J.* **520**, 347 (1999).
- [9] D. C. Black, *Geochim. Cosmochim. Acta* **36**, 347 (1972).
- [10] D. D. Clayton, *Nature (London)* **257**, 36 (1975).
- [11] D. D. Clayton and F. Hoyle, *Astrophys. J.* **187**, L101 (1974).
- [12] A. F. Iyudin *et al.*, *Astron. Astrophys.* **300**, 422 (1995).
- [13] J. Görres *et al.*, *Phys. Rev. C* **39**, 8 (1989).
- [14] S. Seuthe *et al.*, *Nucl. Phys. A* **514**, 471 (1990).
- [15] F. Stegmüller *et al.*, *Nucl. Phys. A* **601**, 168 (1996).
- [16] A. L. Sallaska *et al.*, *Phys. Rev. Lett.* **105**, 152501 (2010).
- [17] K. Peräjärvi *et al.*, *Phys. Lett. B* **492**, 1 (2000).
- [18] V. E. Jacob *et al.*, *Phys. Rev. C* **74**, 045810 (2006).
- [19] A. Saastamoinen *et al.*, *Phys. Rev. C* **83**, 045808 (2011).
- [20] O. S. Kirsebom *et al.*, *Eur. Phys. J. A* **47**, 130 (2011).
- [21] H. Nann *et al.*, *Phys. Rev. C* **23**, 606 (1981).
- [22] S. Kubono *et al.*, *Z. Phys. A* **348**, 59 (1994).
- [23] S. Schmidt *et al.*, *Nucl. Phys. A* **591**, 227 (1995).
- [24] D. G. Jenkins *et al.*, *Phys. Rev. Lett.* **92**, 031101 (2004).
- [25] D. G. Jenkins *et al.*, *Phys. Rev. C* **87**, 064301 (2013).
- [26] K. P. Artemov *et al.*, *Sov. J. Nucl. Phys.* **52**, 408 (1990).
- [27] S. Kubono *et al.*, *Eur. Phys. J. A* **13**, 217 (2002).
- [28] Y. Yanagisawa *et al.*, *Nucl. Instrum. Methods A* **539**, 74 (2005).
- [29] Z. Sun *et al.*, *Nucl. Instrum. Methods A* **503**, 496 (2003).
- [30] J.J. He, S.W. Xu, P. Ma *et al.*, *Nucl. Instrum. Methods A* **680**, 43 (2012).
- [31] S.J. Jin, Y.B. Wang, J. Su *et al.*, *Phys. Rev. C* **88**, 035801 (2013).
- [32] C. Angulo *et al.*, *Nucl. Phys. A* **656**, 3 (1999).